Title:

Dual-specific autophosphorylation of kinase IKK2 enables phosphorylation of substrate IκBα without requiring ATP

Prateeka Borar[1], Tapan Biswas[2], Tom Huxford[3], Gourisankar Ghosh[2] & Smarajit Polley[1,*]

[1]Department of Biological Sciences, Bose Institute, Kolkata, India, [2]Department of Chemistry and Biochemistry, University of California San Diego, La Jolla, USA, [3]Department of Chemistry and Biochemistry, San Diego State University, San Diego, USA.

*Correspondence to be addressed to: spolley@jcbose.ac.in, smarajit.polley@gmail.com

Abstract:

IKK2, a Ser/Thr kinase, acts as a gateway to canonical activation of NF-κB underlying stress signalling. The immediate targets of IKK2 are two serines (S32 and S36) of IκBα, which undergo phosphorylation within minutes of a specific stimuli. Here, we report that IKK2 autophosphorylates itself at tyrosine residues in *cis* in addition to its activation loop serines. Mutation of one such tyrosine, Y169, located in proximity to the active site, to phenylalanine renders IKK2 inactive for phosphorylation of S32 of IκBα. Surprisingly, we observe that auto-phosphorylated IKK2 relayed phosphate group(s) to IκBα even in the absence of ATP if ADP is present. We also observed that mutation of K44, an ATP-binding lysine conserved in all protein kinases, to methionine renders IKK2 inactive towards specific phosphorylation of S32 or S36 of IκBα, but not non-specific substrates. These observations highlight an unusual evolution of IKK2, in which autophosphorylation of tyrosine(s) in the activation loop and the invariant ATP-binding K44 residue are required in defining its substrate specificity for S32,S36 of IκBα. We speculate that this dual specificity may provide the desired specificity to substrate phosphorylation ensuring the fidelity of NF-κB activation.

Introduction:

Inflammatory or pathogenic signals trigger precisely regulated induction of the transcription factor NF-κB in metazoans [1]. This process depends upon the upstream activation of Inhibitor of κB Kinase-complex (IKK-complex), comprising two catalytic subunits, IKK1 (also known as IKKα) and IKK2 (or IKK2β), and an essential regulatory scaffolding protein, NEMO (IKKγ)[2-4]. IKK2 activity is maintained at a very low basal level in resting cells [5-8]. Upon activation, IKK2 phosphorylates the N-terminus of IκBα (Inhibitor of κBα) protein specifically at two Serine residues (S32 and S36) marking it for ubiquitinylation-mediated proteasomal degradation. This liberates NF-κB to execute its gene expression program [6,9-11]. Mutation of both S32 and S36 to alanine residues converts IκBα into a nonphosphorylatable super-repressor of NF-κB[12,13]. Furthermore, IKK possesses exquisite specificity for these two serines, it fails to phosphorylate IκBα when S32 and S36 are mutated even to another phosphorylatable residue, threonine[2].

56 A majority of the eukaryotic protein kinases are Ser/Thr/Tyr kinases (STYKs) that
57 phosphorylate specific namesake residues of their cognate substrates[14,15]. STYKs could
58 specifically phosphorylate S/T or Y[14,16] or S/T as well as Y residues[17,18]. STYKs are rather
59 promiscuous but can display a high substrate specificity in an appropriate context [19]. IKK2 is
60 one such pleotropic kinase that also ensures activation of a particular signaling cascade with
61 fidelity [20,21]. IKK2 toggles between inactive and active states based on phosphorylation status
62 of two serine residues (S177 and S181; S176 and S180 in IKK1) within its activation loop (AL)
63 [22], [23-25]. Replacement of these two serines with phospho-mimetic glutamate residues
64 (S177E,S181E; henceforth EE) renders the kinase constitutively active. IKK2 is reported to be
65 primed through phosphorylation at S177 by the upstream kinase TAK1 that leads to auto-
66 phosphorylation at S181, thus rendering the kinase fully active in cells[26]. However,
67 oligomerization upon association with NEMO, in presence of linear or Lys-63 linked poly-
68 ubiquitin (Ub) chains or at a high concentration, also enables *trans* auto-phosphorylation at
69 S177 and S181 [24,27-29]. Activated IKK2 phosphorylates IκBα specifically at residues S32/S36
70 and the C-terminal SDD (residue range 645-756) is necessary for this [30]. Other sites of IκBα,
71 but not S32/S36, can be phosphorylated by various kinases [31,32]. These findings underscore
72 the ability of IKK2 to function specifically in ensuring rapid NF-κB activation in canonical-
73 signaling. It is, however, still not fully understood how IKK2 achieves its exquisite specificity
74 towards S32/S36 of IκBα and induces NF-κB transcriptional activity.

75 An in-depth analysis of the catalytic features of IKK2 revealed that IKK2 can
76 phosphorylate its own tyrosine residue(s) in addition to its own serines or the serines of its
77 substrate IκBα, i.e., IKK2 possesses dual specificity. This phosphorylation at tyrosine
78 residue(s) is autocatalytic. Furthermore, we observed that, after auto-phosphorylation at
79 tyrosine, IKK2 can phosphorylate IκBα in the absence of ATP, as long as ADP is present in
80 the reaction. Mass spectrometry of IKK2 identified that Y169 and Y188, both present within
81 proximity of the enzyme active site, can undergo auto-phosphorylation in *cis*. This
82 phosphorylation at tyrosine residues is dependent upon the prior activation of IKK2 via AL

83 S177/S181 phosphorylation, and critical to phosphorylation of signal responsive S32/S36 of
84 IκBα. Mutation of Y169 of IKK2 (which has long been associated with pathological conditions
85 such as ectodermal dysplasia) to phenylalanine severely compromised phosphorylation of
86 IκBα at S32. We also found that mutation of the conserved ATP-interacting residue K44 in
87 IKK2 to methionine leads to a loss of Tyr-auto-phosphorylation activity of the kinase and its
88 ability to phosphorylate S32/S36 of IκBα. Interestingly, K44M retained non-specific kinase
89 activity. Overall, our results reveal unique and transient tyrosine phosphoester intermediates
90 of IKK2 that appear to be critical in relaying phosphoryl group(s) specifically to S32/S36 of
91 IκBα, thus ensuring fidelity of NF-κB activation.

92 **Results:**
93
94 ***IKK2 undergoes auto-phosphorylation at uncharacterized sites:*** During our study of IKK2
95 activation, we found increasingly higher levels of IKK2 phosphorylation upon incubation of a
96 recombinant pure IKK2 with radioactive ATP. We surmised that one or multiple residues
97 besides the known phosphorylation sites (S177/181) might also be phosphorylated (**Fig. 1a**
98 and **Fig. 1b**). This phosphorylation of IKK2 did not display any reliance upon the presence of
99 substrate IκBα or NEMO (**Fig. 1c**). To confirm if this phosphorylation of IKK2 is indeed auto-
100 phosphorylation, and not dependent upon another kinase co-purified with IKK2, we generated
101 a K44M mutant of full-length IKK2, which is largely inactive (K44 is a conserved ATP-binding
102 residue in STYK kinases). An *in vitro* kinase assay of IKK2-K44M in absence or presence of
103 wild type (WT) IKK2 using γ^{32}P-ATP as the phospho-donor confirmed that the IKK2-K44M
104 lacked both substrate (IκBα) phosphorylation and auto-phosphorylation activities
105 (**Supplementary Data Fig. 1a**). The auto-phosphorylation is further supported by *in vitro*
106 radioactive kinase assay in the presence or absence of an IKK-specific ATP-competitive
107 inhibitor, Calbiochem Inhibitor VII (**Fig. 1d**).

108 Next, we used various C-terminal (serine-rich region) truncation mutants of the IKK2-
109 EE lacking known phosphorylation sites S177 and S181 [33]. The shortest construct, Δ664EE,
110 lacked the whole flexible C-terminus (665-756); and this was further treated with trypsin to

111 eliminate residues, if any, from the flexible ends of the enzymes prior to *in vitro* kinase assays.
112 All these mutants are found active in auto- and IκBα substrate phosphorylation (**Fig. 1e**). Auto-
113 phosphorylation despite the absence of AL serines and serines within the C-terminus strongly
114 suggested the presence of hitherto uncharacterized phosphorylation sites in IKK2. A striking
115 enhancement in stability of IKK2 upon this auto-phosphorylation is reflected in the change of
116 Tm from ~ 40 °C to ~ 50 °C in differential scanning calorimetry (DSC) scans in the presence
117 of ADP and ATP (**Supplementary Data Fig. 1b**). This behavior tallies with increased solubility
118 of IKK2 observed after auto-phosphorylation that was essential for its successful
119 crystallization[24].
120 ***Auto-phosphorylation of IKK2 reveals dual specificity:*** To test if Tyr residues can undergo
121 auto-phosphorylation in addition to Ser (and Thr), IKK2 incubated with Mg^{2+}-ATP for various
122 time periods was probed with antibodies that specifically recognize AL serines of IKK2 (**Fig.**
123 **2a**, upper panel) or phospho-tyrosine residues (**Fig. 2a**, middle panel). Unexpectedly, we
124 observed *de novo* auto-phosphorylation of IKK2 on tyrosine residues along with the
125 anticipated auto-phosphorylation of AL serines. The tyrosine auto-phosphorylation was
126 abolished in the presence of an IKK-specific inhibitor, Inhibitor VII (**Fig. 2b**). A similar assay
127 was performed to monitor the phospho-tyrosine level in IKK2 as a function of urea
128 concentration. This revealed the detrimental effects of urea at concentrations beyond 1M
129 (**Supplementary Data Fig. 2a**). A more sensitive assay with γ^{32}P-ATP as the phospho-donor
130 also indicated that urea concentrations beyond 1M inhibited both auto-phosphorylation (pan-
131 phosphorylation) and IκBα phosphorylation (**Supplementary Data Fig. 2b**). Furthermore, the
132 IKK2-K44M mutant (kinase inactivating) did not display any tyrosine phosphorylation when
133 incubated with ATP unlike WT IKK2 (**Fig. 2c**). These results confirm novel tyrosine
134 phosphorylation ability of IKK2, demonstrating its dual specificity to both its own Ser and Tyr
135 residues.
136 Next, we checked the requirement of the C-terminal NEMO binding domain (NBD) for
137 autocatalytic dual specificity. Constructs of various truncations (lacking NBD) were capable of

138 phosphorylating IκBα at signal-responsive S32 and S36, and phosphorylating itself on tyrosine
139 residue(s) (**Fig. 2d**). Next, we assessed the autocatalysis at Ser/Thr and Tyr by IKK2 using a
140 constitutively active NBD-truncated version of IKK2 ($IKK2^{\Delta 664}EE$). The protein was recognized
141 by monoclonal anti-p-Ser antibody with or without fresh ATP-treatment as anticipated;
142 however, p-Tyr antibody recognized it strongly only upon fresh ATP-treatment (**Fig. 2e**).

143 To identify tyrosine residues that are phosphorylated *de novo* on IKK2 upon addition
144 of fresh ATP, we performed LC/MS/MS analyses. We identified at least two residues, Y169
145 and Y188, to be phosphorylated upon fresh ATP treatment[34,35] (**Supplementary Data Fig.**
146 **2c,d**). Interestingly, both are located within the AL (**Supplementary Data Fig. 2e**); Y169 is
147 the DFG+1 (DLG in case of IKK2 and IKK1) residue while Y188 (equivalent to Y204 of PKA)
148 is located at the end of AL. It was previously established that DFG+1 position is crucial for
149 defining the substrate specificity of a kinase[36]. Y188 counterpart Y204 of PKA is reported to
150 allosterically modulate PKA activity by altering its conformational entropy[37,38]. We also
151 observed that activity of IKK2 towards S32 and S36 of IκBα and its own tyrosine residue(s)
152 were affected similarly when the kinase assays were performed in the presence of various
153 kinase inhibitors, both general (AMPPNP and Staurosporine) and IKK-specific (MLN-120B,
154 TPCA, Inhibitor VII) (**Supplementary Data Fig. 2f**). These observations confirm that canonical
155 activity of IKK2 towards S32 and S36 of IκBα, and towards its own tyrosine residues are
156 mediated by the same active site pocket.

157 To investigate if Tyr phosphorylation occurs in *cis* (within the same kinase molecule,
158 intramolecular) or *trans* (by a different kinase molecule, intermolecular), we incubated full-
159 length IKK2-K44M with ATP in absence or presence of a constitutively active $IKK2^{\Delta 743}$-EE
160 lacking the extreme C-terminal end. $IKK2^{\Delta 743}$-EE was pre-treated with ATP, and purified
161 through a Superdex200 size-exclusion column to remove unutilized ATP. Absence of p-Tyr
162 signal on $IKK2^{FL}$-K44M irrespective of the presence of $IKK2^{\Delta 743}$-EE, and presence of the p-Tyr
163 signal on the $IKK2^{\Delta 743}$-EE strongly suggested that tyrosine auto-phosphorylation occurs in *cis*,
164 and not in *trans* (**Fig. 2i**, **upper panel**). In contrast, strong phosphorylation of AL S177/S181

165 on the IKK2^{FL}-K44M by IKK2$^{\Delta 743}$-EE suggests that AL serine auto-phosphorylation of IKK2
166 could occur in *trans*, agreeing with our previous findings (**Fig. 2f, middle panel**)[24].
167 To test the effect of phosphorylation at Y169 and Y188, we generated Y169F and
168 Y188F mutants. Radioactive *in vitro* kinase assays using recombinant purified IKK2^{FL}-Y188F
169 and IKK2^{FL}-Y169F mutants revealed drastic reduction in activity of IKK2 (**Fig. 2g**). Since the
170 DFG+1 residue in kinases (Y169 in IKK2) is known to dictate its specificity, we created
171 different mutants of the IκBα substrate where S32 and S36 were singly and independently
172 altered to either alanine (unphosphorylatable) or glutamic acid (phosphomimetic) residues.
173 Mutation of S36 to either Ala or Glu drastically reduced the phosphorylation signal of IκBα
174 while that for the S32A/E mutants were minimally affected (**Fig. 2h**). This suggests that
175 presence of Tyr (and possibly its phosphorylation) is critically important for signal responsive
176 phosphorylation of IκBα. Since pTyr mimic residue is not available, testing roles of modified
177 tyrosine residues is not easily amenable.
178 Next, we tested the consequence of Y169F and Y188F mutants on NF-κB signaling.
179 We reconstituted IKK2 knock-out mouse embryonic fibroblast cells with WT, Y169F and
180 Y188F mutants of IKK2, and measured signal induced activation of IKK2 upon TNF-α
181 treatment. IKK2 activity is significantly reduced in Y169F and nearly abolished in Y188F (**Fig.
182 2i)**. Together these results suggest a communication between the phosphorylation of Y169 of
183 IKK2 and that of S32 of IκBα.
184 ***Freshly auto-phosphorylated IKK2 phosphorylates IκBα in absence of ATP:*** We
185 observed phosphorylation of tyrosine residue(s) by WB or mass spectrometry only upon fresh
186 ATP-treatment, indicating that tyrosines of purified IKK2 loses its phosphate group[39]. It may
187 be noted that, we did not observe any density of phosphates on any of these residues in the
188 human IKK2 crystal structure derived from ATP-treated protein sample[24]. This suggested an
189 intriguing possibility that the phosphate linked to Tyr residue(s) may serve as a temporary
190 phosphate-sink and could eventually be transferred to substrate IκBα. To test this possibility,
191 we first allowed purified IKK2 to undergo auto-phosphorylation by incubating the excess

192 kinase with limiting amounts of radiolabeled γ-^{32}P-ATP followed by two passes through
193 desalting spin columns (40 kDa MW cut off) to remove unreacted ATP. Nucleotide-free auto-
194 phosphorylated IKK2 (P-IKK2) was incubated with IκBα either in absence of nucleotide or with
195 newly added unlabeled nucleotides, and phosphorylation status of the substrate was
196 subsequently monitored by autoradiography after resolving the reaction mixture on an SDS-
197 PAGE (**Fig. 3a**). Transfer of radiolabeled phosphate to IκBα was observed and the transfer
198 was significantly enhanced in the presence of cold ADP (**Fig. 3b**). This phosphotransfer did
199 not show a dependence on ADP concentrations nor did it significantly decrease in the
200 presence of a high concentration of cold ATP. That addition of excess cold ATP did not reduce
201 the extent of IκBα phosphorylation strongly supports transfer of ^{32}P-phosphate from ^{32}P-IKK2
202 to IκBα (**Fig. 3b**) by a relay mechanism with or without involving ADP.

203 We compared available structural models of human IKK2 to investigate whether
204 tyrosine phosphorylation within the activation loop could be supported based on its structural
205 features[23],[24]. We observe distinct conformations of the activation loop containing S177/S181.
206 The structure of IKK2 dimer is asymmetric in which the activation loop of one monomer is
207 largely disordered while that of the other monomer is mostly ordered (PDB id 4KIK)[23]. In the
208 active monomers S177 and S181 are clearly observed. In these active state conformers, the
209 position and conformation of Tyr169 appears to be well-poised for accepting a phosphate from
210 ATP (**Fig. 3c**). A superposition of IKK2 with a pseudo-substrate-bound PKA shows that the
211 hydroxyl of Tyr169 in IKK2 projects toward the γ-phosphate of ATP similarly to the serine
212 hydroxyl on the PKA inhibitor pseudo-substrate[40,41] (**Fig. 3c, Supplementary Data Fig. 3a**).
213 Strikingly, Tyr1238 within the activation loop of a constitutively active oncogenic mutant of
214 RON tyrosine kinase, which is thought to be activated through *trans* auto-phosphorylation
215 under normal conditions, also appears well-poised for auto-phosphorylation in *cis* as the
216 Tyr169 of IKK2[42] (**Supplementary Data Fig. 3b**). These structural observations suggest that
217 it is possible for tyrosine residues within the flexible activation segment to undergo auto-
218 phosphorylation in *cis* and possibly render the kinase with a novel phospho-transfer activity.

219 We undertook a different strategy to further confirm transfer of phosphate from the
220 kinase (and not ATP) to the substrate. We auto-phosphorylated IKK2^{FL}-WT with excess cold
221 ATP and removed the unreacted ATP from the reaction mixture using size-exclusion
222 chromatography on a Superdex200 column (**Fig. 3d**). P-IKK2 eluted at fractions
223 corresponding to MW between 670 and 158 kDa, i.e., much larger than free ATP (**Fig. 3e**).
224 This P-IKK2 protein was incubated with FL IκBα either in presence or absence of ADP for
225 different time periods. A similar reaction in presence of ATP instead of ADP was performed
226 as a positive control. Phosphorylation of S32 and S36 was efficient in presence of 10 and 50
227 μM ADP but absent when ADP was absent in the reaction mixture. Phosphorylation of IκBα
228 in the presence of 50 μM ATP was significantly more robust as anticipated (**Fig. 3f**). The minor
229 detection of IκBα phosphorylation in absence of ADP in the radioactive assay and lack of it in
230 the cold immunoblotting assay (compare lanes marked with arrows in Figs. 3b and 3f) may
231 indicate higher sensitivity of the radio assay. The need of ADP in phosphotransfer prompted
232 us to consider whether the ADP was contaminated with a trace amount of ATP. ESI-MS
233 analysis of 50 μM ADP indicated no peak corresponding to ATP (**Supplementary Data Fig.**
234 **3c**).
235 We performed another phospho-transfer assay that bypasses the need for purification
236 of P-IKK2 from unreacted ATP. In this assay condition ATP should be totally depleted within
237 10-20 min as no detectable enhancement of Tyr phosphorylation level was observed after that
238 (**Supplementary Data Fig. 3d**). Substrate was added to the reaction post-20, 30, and 40 min
239 ATP treatment at 30°C. We observed phosphorylation of the substrate, indicating transfer of
240 phosphate from P-IKK2. Additionally, substrate phosphorylation reduced significantly at 40
241 min preincubation set perhaps hinting at transient nature of transferable phosphates, and its
242 loss prior to addition of the substrate **(Supplementary Data Fig. 3d**). The results of these
243 experiments allowed us to conclude that transiently auto-phosphorylated tyrosine residues are
244 capable of transferring phosphate to the substrate.

245 ***Phosphotransfer from P-IKK2 is critical to fidelity and specificity of IκBα***
246 ***phosphorylation:***
247 We next tested if phosphotransfer is restricted only to the N-terminal signal responsive
248 S32/S36 or to serines of PEST domain as well. Radioactive kinase assay as described earlier
249 was performed with full-length WT and mutant S32A,S36A (AA) IκBα as the phosphate
250 recipient. Phosphate group(s) of P-IKK2 was not transferred to full-length IκBα AA which
251 retains the serines and threonines within its PEST domain (**Fig. 4a**), indicating
252 phosphotransfer only to the N-terminal serines of IκBα. We also tested the effect of AMPPNP,
253 an unhydrolyzable analogue of ATP, on the phosphotransfer, and found no inhibitory effect
254 irrespective of the presence of ADP. This suggests adenine nucleotides poising the kinase for
255 phosphotransfer (**Fig. 4a)**.
256 During our investigation, we noted unusual behavior in the IKK2-K44M mutant. IKK2-
257 K44M phosphorylated full-length WT IκBα robustly but with much less efficiency than WT
258 IKK2. IKK2-K44M also showed a minor auto-phosphorylation activity compared to WT IKK2
259 in the absence of substrate (**Fig. 4b**). We performed a similar kinase assay using full-length
260 WT IκBα where cold ATP was used as the phosphate donor, and phosphorylation status of
261 IκBα at S32,S36 was monitored by immunoblotting. It revealed that IKK2-K44M is unable to
262 phosphorylate S32/S36 (**Fig. 4c**). Since in radioactive kinase assay we observed pan-
263 phosphorylation of the substrate (**Fig. 4b**), it possibly reflects phosphorylation of the PEST
264 region of FL IκBα. We additionally compared IKK2-K44M with WT IKK2 using radioactive
265 kinase assay with both FL IκBα and FL IκBαAA substrates in the absence or presence of
266 Inhibitor VII. As anticipated, FL IκBα was phosphorylated much more efficiently than FL
267 IκBαAA by WT IKK2, and phosphorylation was practically abolished in the presence of 10 μM
268 Inhibitor VII (**Fig. 4d**). In contrast, IKK2-K44M phosphorylated FL IκBαAA more efficiently than
269 FL IκBα, and reduction in the presence of inhibitor VII was strikingly less (**Fig. 4d**). It indicates
270 that IKK2-K44M, despite retaining non-specific kinase activity, lost phosphorylation activity
271 towards S32,S36 of the *bona fide* substrate IκBα. It is noteworthy, an equivalent K to M

272 mutation in Erk2 also didn't abolish the basal activity, but rather retained ~5 % of it[43].

273 **Discussion:**

274 Phosphorylation of substrates by protein kinases is regulated in various ways. IKK2, a kinase
275 central to inflammation, phosphorylates serine residues of its primary substrate IκBα with γ-
276 phosphate ATP. Here, we report multiple intriguing properties of IKK2 that provide specificity
277 to its substrate phosphorylation. These include: 1) autophosphorylation of tyrosine residues
278 of IKK2 in cis, in addition to known auto-phosphorylation at AL serines *i.e.,* dual-specificity; 2)
279 relay of phosphate to substrate IκBα from auto-phosphorylated IKK2 (P-IKK2) either directly
280 or through ADP; and 3) disruption of a universally conserved salt bridge (mediated by K44)
281 renders the kinase non-specific.

282 STYK family of eukaryotic protein kinases transfer γ-phosphate of ATP directly to
283 substrate, in general to S, T and Y residues [44] [41,45-47]. Histidine kinases (in prokaryotes and in
284 some lower eukaryotes) however shuttles the γ-phosphate to Asp residue on a response
285 regulator (RR) substrate through a phospho-His intermediate [48,49] [43,50-52]. Phospho-His
286 functions as a phosphoenzyme intermediate in several metabolic enzymes as well [51]. Our
287 present analyses of eukaryotic protein kinase IKK2 revealed its surprising property in which
288 IKK2 phosphorylated at AL-serines (S177/S181) could be further auto-phosphorylated by ATP
289 at two (Y169 & Y188) or more tyrosine residues (and perhaps other residues) yielding another
290 active form (P-IKK2) (**Fig. 4e**). This marks IKK2 as an autocatalytic dual-specificity kinase
291 rather than a prototype S/T kinase. Interestingly, while auto-phosphorylation at AL-serines
292 (S177 and S181) occurs in *trans* [53], auto-phosphorylation of tyrosine residues occurs in *cis*.
293 This multisite phosphorylated form of IKK2 (P-IKK2) could transfer some of its phosphate(s)
294 to substrate IκBα in presence of ADP without requiring ATP, hinting at an unusual property of
295 IKK2 acting possibly as a phosphate-sink. It is possible that phospho-tyrosines residues of
296 IKK2 act as this sink. The Y169 located at the DFG+1 (DLG in IKK2) position is unique only
297 to IKK1 and IKK2, and is absent even in close mammalian homologues such as IKKε and
298 TBK1. Interestingly, neither IKKε nor TBK1 can phosphorylate IκBα at S32 and S36, *in vitro*

299 or *in vivo*[54,55]. A recent report also indicated the role of DFG+1 residue in differentiating Ser
300 versus Thr residues [36]. These observations hinted to an involvement of Y169 in substrate
301 selectivity. Indeed, our experimental data suggests a pivotal role of Y169 in phosphorylating
302 S32 of IκBα both *in vitro* and ex-vivo (**Fig. 2g-i**). It is worthwhile to note that, an
303 unphosphorylatable mutation at S32 in IκBα to Ile (S32I) is associated with ectodermal
304 dysplasia and T-cell immunodeficiency in patients[56,57]. More interestingly, the placement of
305 this residue in the kinase active site makes it amenable to a phosphorylation-
306 dephosphorylation cycle, suggesting its possible role both in phosphotransfer and substrate
307 specificity. Mutation of Y188, a conserved tyrosine, to unphosphorylatable phenylalanine
308 abolished the kinase activity of IKK2 *in vitro* as well as in MEFs upon TNF-treatment (**Fig. 2g**
309 **and i**). Placement of Y188 indicates that its mutation will be detrimental to the structural fold
310 of kinase, thus it is unclear if or how Y188 plays a role in the phosphor transfer. Since
311 phosphotransfer to S32,S36 of IκBα is observed with auto-phosphorylated IKK2 EE,
312 transferred phosphates are not from S177 or S181.

313 The strength of input signal, level of IκBα degradation, and NF-κB activation correlate
314 with the amplitude, duration, and kinetics of IKK activity [58,59]. This digital (all-or-none) activation
315 profile of NF-κB appears to be due to rapid activation and inactivation of IKK2. IKK targets
316 multiple substrates *in vivo*; however, the rapid activation of NF-κB is regulated primarily by
317 IκBα. How IKK specifically selects IκBα for phosphorylation is unclear, although NEMO is
318 reported to direct the kinase activity of IKK2 specifically towards IκBα [60]. We observe that P-
319 IKK2 could transfer phosphate(s) specifically to the S32/S36 of IκBα, and not to other sites
320 (such as PEST sequence of IκBα) (**Fig. 3b, f and 4a**). We surmise if transiency of multisite
321 phosphorylated IKK2 (P-IKK2) underlie this rapid activation-inactivation events during signal
322 response. It is possible that regulatory system of IKK2 is somewhat analogous the two-
323 component histidine kinase-effector systems in prokaryotes that show a threshold activation
324 response[61 62,63].

325 All three tyrosines in AL of IKK2 are previously reported to undergo signal-induced
326 phosphorylation in cells. These modifications were proposed to be mediated by a tyrosine
327 kinase although there is no evidence of a specific tyrosine kinase [35,64,65]. Several members of
328 the Ser/Thr kinase family undergo tyrosine phosphorylation and these kinases employ diverse
329 mechanisms for auto-phosphorylation[66-71].

330 The phosphotransfer from P-IKK2 to IκBα appears inefficient as no apparent decrease
331 in phospho-label in P-IKK2 is observed post transfer (**Fig. 3b**). This is in contrast to HKs where
332 a single phosphate from the phosphorylated HK is stoichiometrically transferred to the cognate
333 RR. There are also other prominent differences, such as phosphorylation on IKK2 occurs at
334 multiple sites unlike at single site for the HKs, and not every phosphorylated residue in P-IKK2
335 expected to transfer its phosphate to IκBα. It is likely that, there are more than one type of
336 phosphorylated residues in P-IKK2 with respect to their stability wherein only a fraction of the
337 total pool can be relayed. Another notable difference between phosphorelay in IKK2 from that
338 in HK is IKK2's dependence on ADP (**Fig. 3b and f**). It was also observed that, the generic
339 kinase inhibitor AMPPNP (unhydrolyzable ATP analogue) failed to inhibit phosphor-transfer
340 from IKK2 (**Fig. 4a**) and IκBα phosphorylation (**Supplementary Data Fig. 2f**). Taken together,
341 we surmise that presence of ADP or AMPPNP help IKK2 attain conformational state poised
342 for phosphorylating S32/36 of IκBα even in absence of ATP. The list of Ser/Thr kinase family
343 proteins that undergo tyrosine phosphorylation is growing that employ diverse mechanisms
344 for auto-phosphorylation[66-71]. The most notable example of this dual specificity is the DYRK.
345 However, the role of Tyr-phosphorylation in DYRK is not related to that in IKK2, nor does it
346 render DYRKs capable of relaying phosphates to the substrates. It will be interesting to see
347 whether phosphotransfer by relay (with or without ADP) occurs in any other kinase-substrate
348 system other than IKK2: IκBα system described here.

349 Our study reveals tyrosine auto-phosphorylation in IKK2 and indicates that
350 consequences of Ser and Tyr autophosphorylations in dual-specific IKK2 are distinct.
351 Moreover, positions of the critical tyrosine residues are unique, such that some that are

352 amenable to *cis* auto-phosphorylation are essential for substrate phosphorylation. Most
353 surprisingly, the tyrosine-linked phosphate groups can be transferred by a relay-mechanism
354 to specific serines in IκBα, an event reminiscing phospho-relay in two component systems
355 prevalent in prokaryotes and some lower eukaryotes. Our study also reveals the role of K44
356 of IKK2 in auto-phosphorylation and thus in specific phosphorylation of S32,S36 of IκBα,
357 although it does not affect its non-specific kinase activity. It requires further investigation to
358 determine if a structural state of IKK2, perhaps through a different modification or through
359 binding to another protein, allow it to phosphorylate substrates relatively non-specifically.

360 In all, it is intriguing how the gateway to the activation of NF-κB is regulated through
361 unique phosphorylation events in IKK2 (**Fig. 4f**). It appears that a multi-layered fail-safe
362 mechanism is devised to tightly control NF-κB activation. Firstly, in absence of upstream
363 signals IKK-complex is unable to phosphorylate Ser 32,36 of IκBα efficiently thereby keeping
364 check on the aberrant and untimely activation of NF-κB. Upon proinflammatory cues cells
365 need to activate NF-κB immediately and efficiently, i.e., IKK needs to be activated and
366 phosphorylate Ser 32,36 of IκBα. NEMO warrants IKK-activation and ensures that the IKK-
367 complex specifically chooses IκBα from a large pool of substrates of IKK2. IKK2 is designed
368 in such a manner that it phosphorylates itself at AL-tyrosines when activated, such that
369 phosphate group(s) can be relayed directly or through ADP to Ser32,36 of IκBα with great
370 fidelity, thus leaving little chance of a misconstrued signaling event thereby confirming NF-κB
371 activation. Our discovery might also present the beginning of a new aspect in eukaryotic cell-
372 signaling by EPKs and provide a foundation for mechanistic studies of an intriguing phospho-
373 transfer reaction that helps accomplish the desired specificity. To the best of our knowledge,
374 it is the first report to strongly suggest that a metazoan EPK harbors HK-like phosphotransfer
375 activity through relay mechanism to its substrate.

376 **Acknowledgement:** We thank Joe Adams and Simpson Joseph (UCSD), Tony Hunter (Salk
377 Institute) and Alex Hoffmann (UCLA) for commenting on the work. Authors also thank
378 members of Polley lab (BI) and Ghosh Lab (UCSD) for their continuous support. We also

thank Majid Ghassemian (Biomolecular Mass spectrometry facility, UCSD) and Souvik Roy (Mass spectrometry facility, BI) for the mass spectrometry experiments and analyses. This work was supported by an Intermediate Fellowship from the DBT Wellcome Trust India Alliance (IA/I/15/1/501852) & intramural funding from Bose Institute to SP, NIH grant to GG and American Cancer Society grant RSG-08-287-01-GMC to TH. Biochemistry research at SDSU is supported in part by the California Metabolic Research Foundation. PB was supported by the graduate research fellowship from Bose Institute.

Author contribution: SP, GG and TB designed experiments; PB, SP, TB & GG performed experiments. SP, GG, TB, TH and PB analyzed the results. SP wrote the manuscript with the help of PB and TB in preparing figures and images, GG, TB and TH modified the manuscript.

Ethics declarations:

Competing interests: The authors declare no competing financial interests.

393 **References**

394 1 Hoffmann, A. & Baltimore, D. Circuitry of nuclear factor kappaB signaling. *Immunol*
395 *Rev* **210**, 171-186, doi:10.1111/j.0105-2896.2006.00375.x (2006).

396 2 DiDonato, J. A., Hayakawa, M., Rothwarf, D. M., Zandi, E. & Karin, M. A cytokine-
397 responsive IkappaB kinase that activates the transcription factor NF-kappaB. *Nature*
398 **388**, 548-554, doi:10.1038/41493 (1997).

399 3 Zandi, E., Rothwarf, D. M., Delhase, M., Hayakawa, M. & Karin, M. The IkappaB kinase
400 complex (IKK) contains two kinase subunits, IKKalpha and IKKbeta, necessary for
401 IkappaB phosphorylation and NF-kappaB activation. *Cell* **91**, 243-252 (1997).

402 4 Rothwarf, D. M., Zandi, E., Natoli, G. & Karin, M. IKK-gamma is an essential regulatory
403 subunit of the IkappaB kinase complex. *Nature* **395**, 297-300, doi:10.1038/26261
404 (1998).

405 5 Hacker, H. & Karin, M. Regulation and function of IKK and IKK-related kinases. *Sci*
406 *STKE* **2006**, re13, doi:10.1126/stke.3572006re13 (2006).

407 6 Hinz, M. & Scheidereit, C. The IkappaB kinase complex in NF-kappaB regulation and
408 beyond. *EMBO Rep* **15**, 46-61, doi:10.1002/embr.201337983 (2014).

409 7 Ghosh, S. & Karin, M. Missing pieces in the NF-kappaB puzzle. *Cell* **109 Suppl**, S81-
410 96 (2002).

411 8 Liu, F., Xia, Y., Parker, A. S. & Verma, I. M. IKK biology. *Immunol Rev* **246**, 239-253,
412 doi:10.1111/j.1600-065X.2012.01107.x (2012).

413 9 Scheidereit, C. IkappaB kinase complexes: gateways to NF-kappaB activation and
414 transcription. *Oncogene* **25**, 6685-6705, doi:10.1038/sj.onc.1209934 (2006).

415 10 Karin, M. & Ben-Neriah, Y. Phosphorylation meets ubiquitination: the control of NF-
416 [kappa]B activity. *Annu Rev Immunol* **18**, 621-663,
417 doi:10.1146/annurev.immunol.18.1.621 (2000).

418 11 Hayden, M. S. & Ghosh, S. Shared principles in NF-kappaB signaling. *Cell* **132**, 344-
419 362, doi:10.1016/j.cell.2008.01.020 (2008).

420 12 Brown, K., Gerstberger, S., Carlson, L., Franzoso, G. & Siebenlist, U. Control of I
421 kappa B-alpha proteolysis by site-specific, signal-induced phosphorylation. *Science*
422 **267**, 1485-1488, doi:10.1126/science.7878466 (1995).

423 13 Lin, Y. C., Brown, K. & Siebenlist, U. Activation of NF-kappa B requires proteolysis of
424 the inhibitor I kappa B-alpha: signal-induced phosphorylation of I kappa B-alpha alone
425 does not release active NF-kappa B. *Proc Natl Acad Sci U S A* **92**, 552-556,
426 doi:10.1073/pnas.92.2.552 (1995).

427 14 Manning, G., Whyte, D. B., Martinez, R., Hunter, T. & Sudarsanam, S. The protein
428 kinase complement of the human genome. *Science* **298**, 1912-1934,
429 doi:10.1126/science.1075762 (2002).

430 15 Manning, G., Plowman, G. D., Hunter, T. & Sudarsanam, S. Evolution of protein kinase
431 signaling from yeast to man. *Trends Biochem Sci* **27**, 514-520, doi:10.1016/s0968-
432 0004(02)02179-5 (2002).

433 16 Dhanasekaran, N. & Premkumar Reddy, E. Signaling by dual specificity kinases.
434 *Oncogene* **17**, 1447-1455, doi:10.1038/sj.onc.1202251 (1998).

435 17 He, X., Jones, M. H., Winey, M. & Sazer, S. Mph1, a member of the Mps1-like family
436 of dual specificity protein kinases, is required for the spindle checkpoint in S. pombe.
437 *J Cell Sci* **111 (Pt 12)**, 1635-1647, doi:10.1242/jcs.111.12.1635 (1998).

438 18 Lauze, E. *et al.* Yeast spindle pole body duplication gene MPS1 encodes an essential
439 dual specificity protein kinase. *EMBO J* **14**, 1655-1663, doi:10.1002/j.1460-
440 2075.1995.tb07154.x (1995).

441 19 Ubersax, J. A. & Ferrell, J. E., Jr. Mechanisms of specificity in protein phosphorylation.
442 *Nat Rev Mol Cell Biol* **8**, 530-541, doi:10.1038/nrm2203 (2007).

443 20 Schrofelbauer, B. & Hoffmann, A. How do pleiotropic kinase hubs mediate specific
444 signaling by TNFR superfamily members? *Immunol Rev* **244**, 29-43,
445 doi:10.1111/j.1600-065X.2011.01060.x (2011).

446 21 Antonia, R. J., Hagan, R. S. & Baldwin, A. S. Expanding the View of IKK: New
447 Substrates and New Biology. *Trends Cell Biol* **31**, 166-178,
448 doi:10.1016/j.tcb.2020.12.003 (2021).

449 22 Huse, M. & Kuriyan, J. The conformational plasticity of protein kinases. *Cell* **109**, 275-
450 282, doi:10.1016/s0092-8674(02)00741-9 (2002).

451 23 Liu, S. *et al.* Crystal structure of a human IkappaB kinase beta asymmetric dimer. *J*
452 *Biol Chem* **288**, 22758-22767, doi:10.1074/jbc.M113.482596 (2013).

453 24 Polley, S. *et al.* A structural basis for IkappaB kinase 2 activation via oligomerization-
454 dependent trans auto-phosphorylation. *PLoS Biol* **11**, e1001581,
455 doi:10.1371/journal.pbio.1001581 (2013).

456 25 Xu, G. *et al.* Crystal structure of inhibitor of kappaB kinase beta. *Nature* **472**, 325-330,
457 doi:10.1038/nature09853 (2011).

458 26 Zhang, J., Clark, K., Lawrence, T., Peggie, M. W. & Cohen, P. An unexpected twist to
459 the activation of IKKbeta: TAK1 primes IKKbeta for activation by autophosphorylation.
460 *Biochem J* **461**, 531-537, doi:10.1042/BJ20140444 (2014).

461 27 Du, M., Ea, C. K., Fang, Y. & Chen, Z. J. Liquid phase separation of NEMO induced
462 by polyubiquitin chains activates NF-kappaB. *Mol Cell* **82**, 2415-2426 e2415,
463 doi:10.1016/j.molcel.2022.03.037 (2022).

464 28 Ea, C. K., Deng, L., Xia, Z. P., Pineda, G. & Chen, Z. J. Activation of IKK by TNFalpha
465 requires site-specific ubiquitination of RIP1 and polyubiquitin binding by NEMO. *Mol*
466 *Cell* **22**, 245-257, doi:10.1016/j.molcel.2006.03.026 (2006).

467 29 Chen, Z. J. Ubiquitination in signaling to and activation of IKK. *Immunol Rev* **246**, 95-
468 106, doi:10.1111/j.1600-065X.2012.01108.x (2012).

469 30 Shaul, J. D., Farina, A. & Huxford, T. The human IKKbeta subunit kinase domain
470 displays CK2-like phosphorylation specificity. *Biochem Biophys Res Commun* **374**,
471 592-597, doi:10.1016/j.bbrc.2008.07.082 (2008).

472 31 Barroga, C. F., Stevenson, J. K., Schwarz, E. M. & Verma, I. M. Constitutive
473 phosphorylation of I kappa B alpha by casein kinase II. *Proc Natl Acad Sci U S A* **92**,
474 7637-7641, doi:10.1073/pnas.92.17.7637 (1995).

475 32 Tergaonkar, V., Bottero, V., Ikawa, M., Li, Q. & Verma, I. M. IkappaB kinase-
476 independent IkappaBalpha degradation pathway: functional NF-kappaB activity and
477 implications for cancer therapy. *Mol Cell Biol* **23**, 8070-8083 (2003).

478 33 Zandi, E., Chen, Y. & Karin, M. Direct phosphorylation of IkappaB by IKKalpha and
479 IKKbeta: discrimination between free and NF-kappaB-bound substrate. *Science* **281**,
480 1360-1363, doi:10.1126/science.281.5381.1360 (1998).

481 34 Darwech, I., Otero, J. E., Alhawagri, M. A. & Abu-Amer, Y. Tyrosine phosphorylation
482 is required for IkappaB kinase-beta (IKKbeta) activation and function in
483 osteoclastogenesis. *J Biol Chem* **285**, 25522-25530, doi:10.1074/jbc.M110.121533
484 (2010).

485 35 Otero, J. E. *et al.* Defective osteoclastogenesis by IKKbeta-null precursors is a result
486 of receptor activator of NF-kappaB ligand (RANKL)-induced JNK-dependent apoptosis
487 and impaired differentiation. *J Biol Chem* **283**, 24546-24553,
488 doi:10.1074/jbc.M800434200 (2008).

489 36 Chen, C. *et al.* Identification of a major determinant for serine-threonine kinase
490 phosphoacceptor specificity. *Mol Cell* **53**, 140-147, doi:10.1016/j.molcel.2013.11.013
491 (2014).

492 37 Ahuja, L. G., Kornev, A. P., McClendon, C. L., Veglia, G. & Taylor, S. S. Mutation of a
493 kinase allosteric node uncouples dynamics linked to phosphotransfer. *Proc Natl Acad*
494 *Sci U S A* **114**, E931-E940, doi:10.1073/pnas.1620667114 (2017).

495 38 Yang, J. *et al.* Allosteric network of cAMP-dependent protein kinase revealed by
496 mutation of Tyr204 in the P+1 loop. *J Mol Biol* **346**, 191-201,
497 doi:10.1016/j.jmb.2004.11.030 (2005).

498 39 Eckhart, W., Hutchinson, M. A. & Hunter, T. An activity phosphorylating tyrosine in
499 polyoma T antigen immunoprecipitates. *Cell* **18**, 925-933, doi:10.1016/0092-
500 8674(79)90205-8 (1979).

501 40 Knighton, D. R. *et al.* Structure of a peptide inhibitor bound to the catalytic subunit of
502 cyclic adenosine monophosphate-dependent protein kinase. *Science* **253**, 414-420,
503 doi:10.1126/science.1862343 (1991).

504 41 Nolen, B., Taylor, S. & Ghosh, G. Regulation of protein kinases; controlling activity
505 through activation segment conformation. *Mol Cell* **15**, 661-675,
506 doi:10.1016/j.molcel.2004.08.024 (2004).

507 42 Wang, J. *et al.* The crystal structure of a constitutively active mutant RON kinase
508 suggests an intramolecular autophosphorylation hypothesis. *Biochemistry* **49**, 7972-
509 7974, doi:10.1021/bi100409w (2010).

510 43 Robbins, D. J. *et al.* Regulation and properties of extracellular signal-regulated protein
511 kinases 1 and 2 in vitro. *J Biol Chem* **268**, 5097-5106 (1993).

512 44 Hunter, T. Protein kinase classification. *Methods Enzymol* **200**, 3-37,
513 doi:10.1016/0076-6879(91)00125-g (1991).

514 45 Cohen, P. The origins of protein phosphorylation. *Nat Cell Biol* **4**, E127-130,
515 doi:10.1038/ncb0502-e127 (2002).

516 46 Fischer, E. H. & Krebs, E. G. Conversion of phosphorylase b to phosphorylase a in
517 muscle extracts. *J Biol Chem* **216**, 121-132 (1955).

518 47 Krebs, E. G. & Fischer, E. H. Phosphorylase activity of skeletal muscle extracts. *J Biol*
519 *Chem* **216**, 113-120 (1955).

520 48 Borkovich, K. A. & Simon, M. I. The dynamics of protein phosphorylation in bacterial
521 chemotaxis. *Cell* **63**, 1339-1348, doi:10.1016/0092-8674(90)90429-i (1990).

522 49 Gao, R. & Stock, A. M. Biological insights from structures of two-component proteins.
523 *Annu Rev Microbiol* **63**, 133-154, doi:10.1146/annurev.micro.091208.073214 (2009).

524 50 Hunter, T. A journey from phosphotyrosine to phosphohistidine and beyond. *Mol Cell*
525 **82**, 2190-2200, doi:10.1016/j.molcel.2022.05.007 (2022).

526 51 Kalagiri, R. & Hunter, T. The many ways that nature has exploited the unusual
527 structural and chemical properties of phosphohistidine for use in proteins. *Biochem J*
528 **478**, 3575-3596, doi:10.1042/BCJ20210533 (2021).

529 52 Laub, M. T., Biondi, E. G. & Skerker, J. M. Phosphotransfer profiling: systematic
530 mapping of two-component signal transduction pathways and phosphorelays.
531 *Methods Enzymol* **423**, 531-548, doi:10.1016/S0076-6879(07)23026-5 (2007).

532 53 Pike, A. C. *et al.* Activation segment dimerization: a mechanism for kinase
533 autophosphorylation of non-consensus sites. *EMBO J* **27**, 704-714,
534 doi:10.1038/emboj.2008.8 (2008).

535 54 Larabi, A. *et al.* Crystal structure and mechanism of activation of TANK-binding kinase
536 1. *Cell Rep* **3**, 734-746, doi:10.1016/j.celrep.2013.01.034 (2013).

537 55 Tu, D. *et al.* Structure and ubiquitination-dependent activation of TANK-binding kinase
538 1. *Cell Rep* **3**, 747-758, doi:10.1016/j.celrep.2013.01.033 (2013).

539 56 Mooster, J. L. *et al.* Defective lymphoid organogenesis underlies the immune
540 deficiency caused by a heterozygous S32I mutation in IkappaBalpha. *J Exp Med* **212**,
541 185-202, doi:10.1084/jem.20140979 (2015).

542 57 Courtois, G. *et al.* A hypermorphic IkappaBalpha mutation is associated with
543 autosomal dominant anhidrotic ectodermal dysplasia and T cell immunodeficiency. *J*
544 *Clin Invest* **112**, 1108-1115, doi:10.1172/JCI18714 (2003).

545 58 Cheong, R. *et al.* Transient IkappaB kinase activity mediates temporal NF-kappaB
546 dynamics in response to a wide range of tumor necrosis factor-alpha doses. *J Biol*
547 *Chem* **281**, 2945-2950, doi:10.1074/jbc.M510085200 (2006).

548 59 Behar, M. & Hoffmann, A. Tunable signal processing through a kinase control cycle:
549 the IKK signaling node. *Biophys J* **105**, 231-241, doi:10.1016/j.bpj.2013.05.013 (2013).

550 60 Schrofelbauer, B., Polley, S., Behar, M., Ghosh, G. & Hoffmann, A. NEMO ensures
551 signaling specificity of the pleiotropic IKKbeta by directing its kinase activity toward
552 IkappaBalpha. *Mol Cell* **47**, 111-121, doi:10.1016/j.molcel.2012.04.020 (2012).

553 61 Lamarche, M. G., Wanner, B. L., Crepin, S. & Harel, J. The phosphate regulon and
554 bacterial virulence: a regulatory network connecting phosphate homeostasis and
555 pathogenesis. *FEMS Microbiol Rev* **32**, 461-473, doi:10.1111/j.1574-
556 6976.2008.00101.x (2008).

557 62 Bhate, M. P., Molnar, K. S., Goulian, M. & DeGrado, W. F. Signal transduction in
558 histidine kinases: insights from new structures. *Structure* **23**, 981-994,
559 doi:10.1016/j.str.2015.04.002 (2015).

560 63 Laub, M. T. & Goulian, M. Specificity in two-component signal transduction pathways.
561 *Annu Rev Genet* **41**, 121-145, doi:10.1146/annurev.genet.41.042007.170548 (2007).

562 64 Rieke, C., Papendieck, A., Sokolova, O. & Naumann, M. Helicobacter pylori-induced
563 tyrosine phosphorylation of IKKbeta contributes to NF-kappaB activation. *Biol Chem*
564 **392**, 387-393, doi:10.1515/BC.2011.029 (2011).

565 65 Meyer, A. N. *et al.* Tyrosine phosphorylation allows integration of multiple signaling
566 inputs by IKKbeta. *PLoS One* **8**, e84497, doi:10.1371/journal.pone.0084497 (2013).

567 66 Lochhead, P. A. Protein kinase activation loop autophosphorylation in cis: overcoming
568 a Catch-22 situation. *Sci Signal* **2**, pe4, doi:10.1126/scisignal.254pe4 (2009).

569 67 Lochhead, P. A. *et al.* A chaperone-dependent GSK3beta transitional intermediate
570 mediates activation-loop autophosphorylation. *Mol Cell* **24**, 627-633,
571 doi:10.1016/j.molcel.2006.10.009 (2006).

572 68 Lochhead, P. A., Sibbet, G., Morrice, N. & Cleghon, V. Activation-loop
573 autophosphorylation is mediated by a novel transitional intermediate form of DYRKs.
574 *Cell* **121**, 925-936, doi:10.1016/j.cell.2005.03.034 (2005).

575 69 Bhattacharyya, R. P. *et al.* The Ste5 scaffold allosterically modulates signaling output
576 of the yeast mating pathway. *Science* **311**, 822-826, doi:10.1126/science.1120941
577 (2006).

578 70 Tigno-Aranjuez, J. T., Asara, J. M. & Abbott, D. W. Inhibition of RIP2's tyrosine kinase
579 activity limits NOD2-driven cytokine responses. *Genes Dev* **24**, 2666-2677,
580 doi:10.1101/gad.1964410 (2010).

581 71 Ge, B. *et al.* MAPKK-independent activation of p38alpha mediated by TAB1-
582 dependent autophosphorylation of p38alpha. *Science* **295**, 1291-1294,
583 doi:10.1126/science.1067289 (2002).
584
585

Figure 1

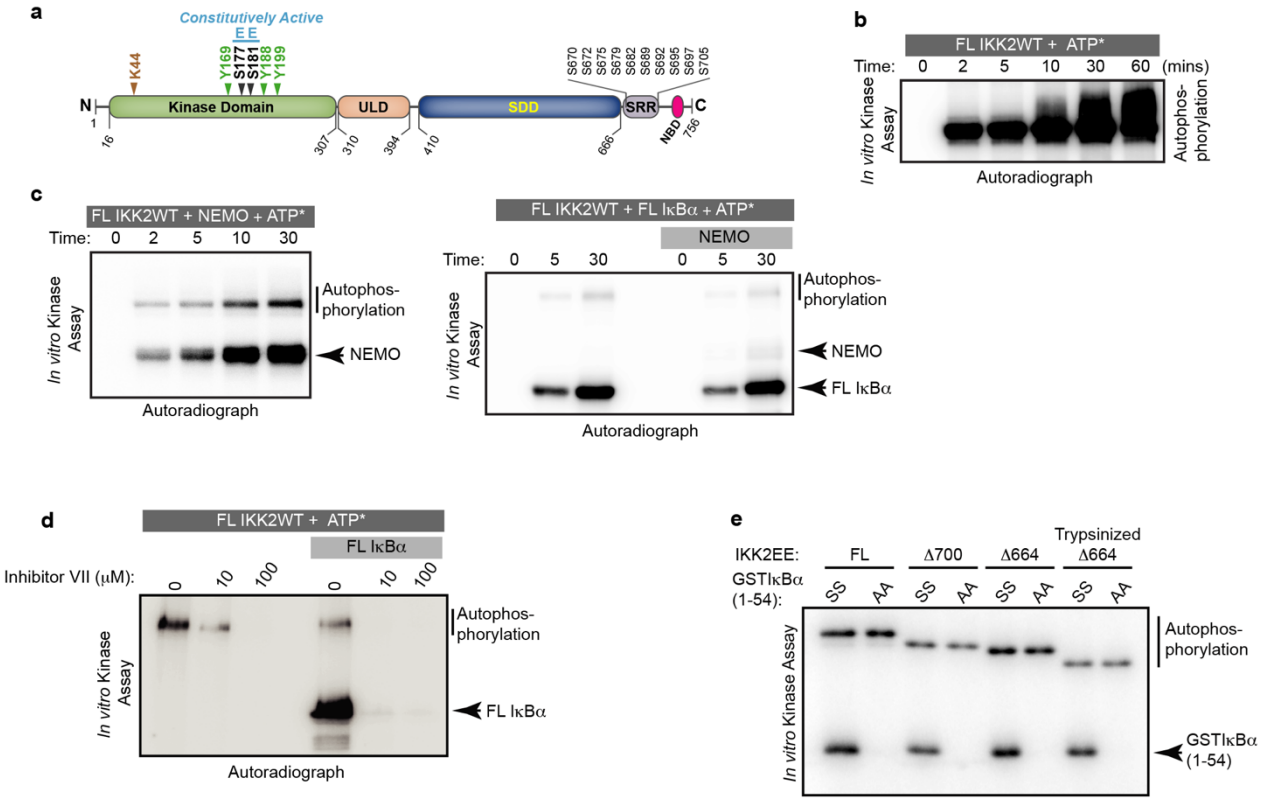

Figure 1: Autophosphorylation of IKK2 at hitherto uncharacterized sites. a) Domain organisation of FL IKK2 depicting functional kinase domain (KD), ubiquitin-like domain (ULD), and scaffold dimerization domain (SDD) based on the X-ray structures. Known sites of Ser phosphorylation and NEMO interacting regions at the extreme C-termini are highlighted. Serine and tyrosine residues in the activation loop are shown, mutation of which to Glu renders IKK2 constitutively active. The conserved ATP-interacting Lys (at position 44) is also shown. **b)** Autophosphorylation of FL IKK2WT upon incubation with radioactive ATP for different time periods in an *in vitro* kinase assay. **c)** *In vitro* radioactive kinase assays performed to check the effect of NEMO on autophosphorylation of FL IKK2WT (left panel), and that of NEMO and IκBα on autophosphorylation and substrate phosphorylation (right panel) activity of FL IKK2WT. **d)** Effect of Inhibitor VII on FL IKK2WT autophosphorylation and IκBα substrate phosphorylation at different inhibitor concentrations by in a radioactive *in vitro* kinase assay. **e)** Radioactive kinase assay conducted to check auto- and substrate phosphorylation of full length and deletion constructs of constitutively active form of IKK2 harbouring

Figure 2

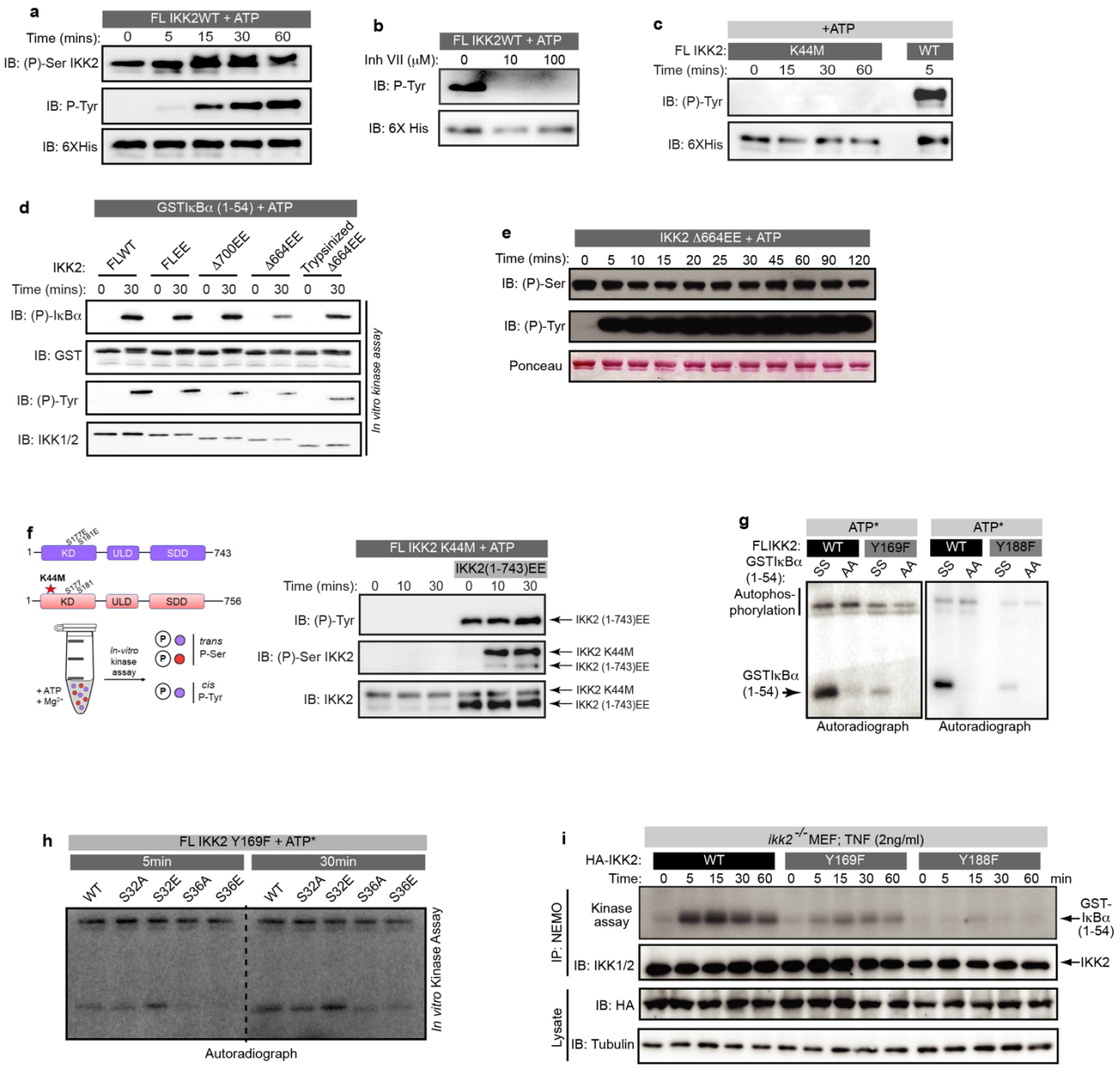

Figure 2: IKK2 possesses autocatalytic dual specificity. a) *In vitro* kinase assay followed by immunoblotting with FL IKK2WT against phospho Ser (177/181) and phospho-Tyr antibodies. **b)** Effect of Inhibitor VII on tyrosine autophosphorylation of FL IKK2WT. **c)** Immunoblotting performed with phospho-Tyr antibody to check autophosphorylation of IKK2 mutant K44M at different time points compared to that of IKK2 WT. **d)** Tyrosine auto phosphorylation and substrate phosphorylation of GST (1-54) IκBα in presence of full length and deletion mutants of IKK2 harbouring phosphomimetic Ser177Glu and Ser181Glu mutations. **e)** *De novo* Auto-phosphorylation of IKK2 on tyrosine monitored by phospho-Ser and phospho-Tyr specific monoclonal antibodies. **f)** *In vitro* kinase assay followed by immunoblotting done showing active IKK2 cannot phosphorylate tyrosines of an inactive (K44M) IKK2 mutant; however, can efficiently phosphorylate AL serines. **g)** Radioactive *in vitro* kinase assay performed with IKK2 Y169F and Y188F mutants using GST (1-54) IκBα WT and AA as substrates. **h)** Radioactive *in vitro* kinase assay performed with IKK2 Y169F mutant with a range of GST (1-54) IκBα mutants where the substrate phosphorylation signal is abolished in case of S36 A/E IκBα. **i)** Severe reduction in TNFα-induced IKK activity in *ikk2-/-* MEF-3T3 cells reconstituted with mutant (Y169F and Y188F) IKK2s compared to wild-type. Kinase assay was performed with IKK immunoprecipitated (IP-ed) with anti-NEMO antibody from whole cell extract.

Figure 3

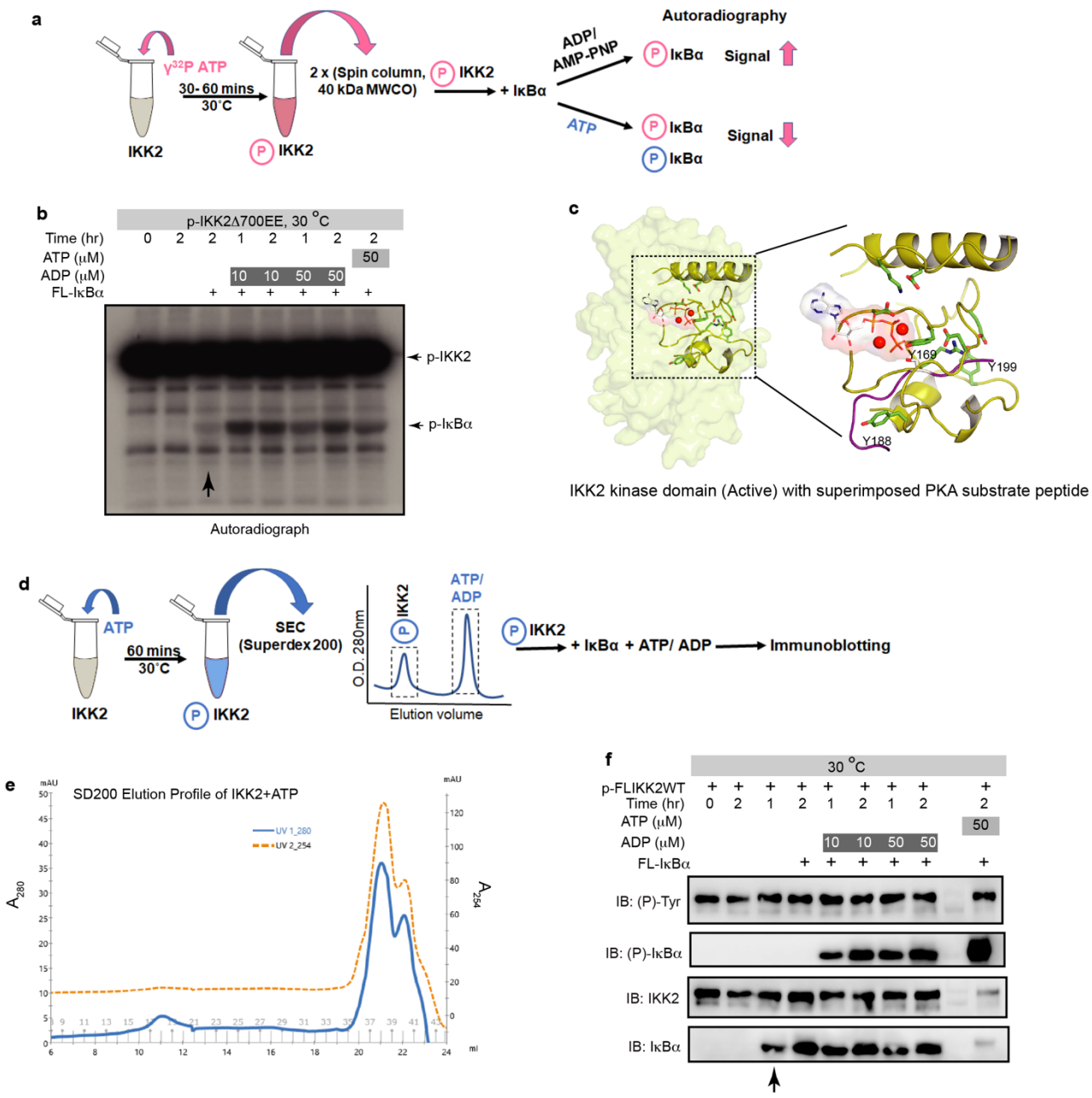

Figure 3: Freshly autophosphorylated IKK2 relays phosphates to IκBα. a) Schematic representation of the experiment performed to monitor the path traversed by phosphate(s) from p-IKK2 to substrate by autoradiography detection method. **b)** Purified autophosphorylated (radiolabelled) IKK2 transfers its phosphate to IκBα substrate in absence of any nucleotide, and transfer efficiency is enhanced upon addition of ADP or ATP. **c)** A close-up view of the active site in active form in the context of the entire kinase domain. Three tyrosines (Y169, Y188 and Y199) in immediate vicinity of active sites are highlighted. Position of ATP is modelled based on the structure of PKA. **d)** Schematic representation of the experiment performed to monitor the path traversed by phosphate(s) from p-IKK2 to substrate by immunoblotting detection method. **e)** Elution profile of the size exclusion chromatography run of p-IKK2 to get rid of excess unlabelled ATP performed in Superdex200 10/30 increase. **f)** Purified autophosphorylated (cold) IKK2 transfers its phosphate to IκBα substrate with enhanced transfer efficiency upon addition of ADP or ATP.

Figure 4

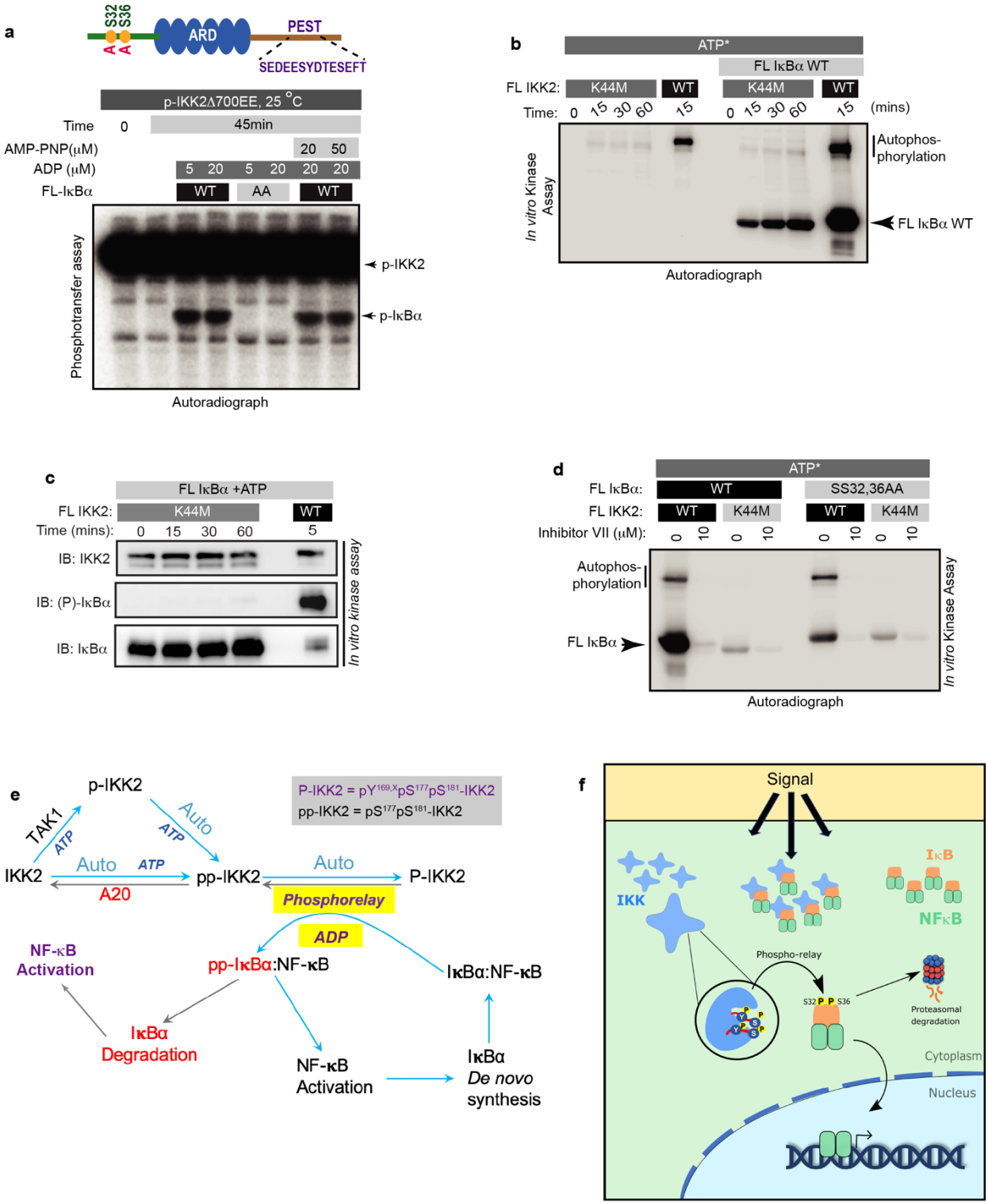

Figure 4: Specificity and fidelity of phosphorelay by IKK2 to IκBα. a) AMP-PNP can support efficient phosphorelay. Phospho-relay reaction is observed in IκBα WT but not in S32,36Ala double mutant. Domain organization and position of relevant S/T/Y residues of IκBα are shown above the autoradiograph. **b)** Comparison of kinase activity of FL IKK2WT and K44M mutant phosphorylation signal compared to that of IKK2 WT in radioactive kinase assay performed with FL IκBα WT as the substrate. **c)** Residue level specificity of phosphorylation by the FL IKK2K44M was analysed using an antibody that specifically phosphor-S32/36 of IκBα. **d)** Differential sensitivity of specific vs. non-specific phosphorylation by IKK2 as assessed by the effect of Inhibitor VII on FL IKK2 WT and IKK2 K44M using IκBα WT and AA as substrates. **e)** A detailed scheme of reactions showing IKK2-activation and subsequent phosphorylation of the signal responsive S32,36 on IκBα by phosphorelay. **f)** A cartoon representation of the proposed model of NF-kB activation by IKK2 employing phosphorelay to IκBα.

Figure S1

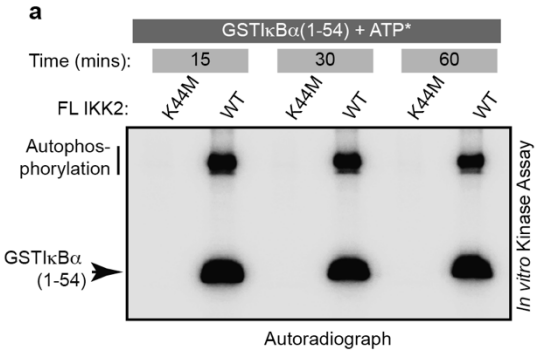

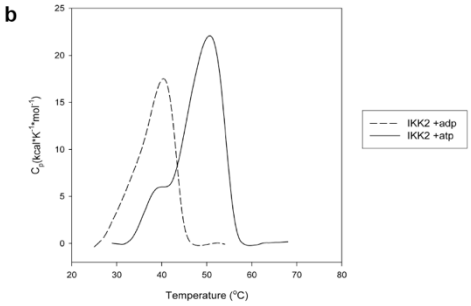

Sample	T_m (°C)	ΔH (Kcal/mol)
IKK2+ADP	40.1	164.0
IKK2+ATP	50.8	251.9

Supplementary Figure 1: a, Autoradiograph of *in vitro* kinase assay reactions carried out with FL IKK2WT and K44M using GST (1-54) IκBα as the substrate as a function of time. **b,** A differential scanning calorimetry (DSC) thermogram showing a striking enhancement in folding stability of IKK2 upon ATP-treatment.

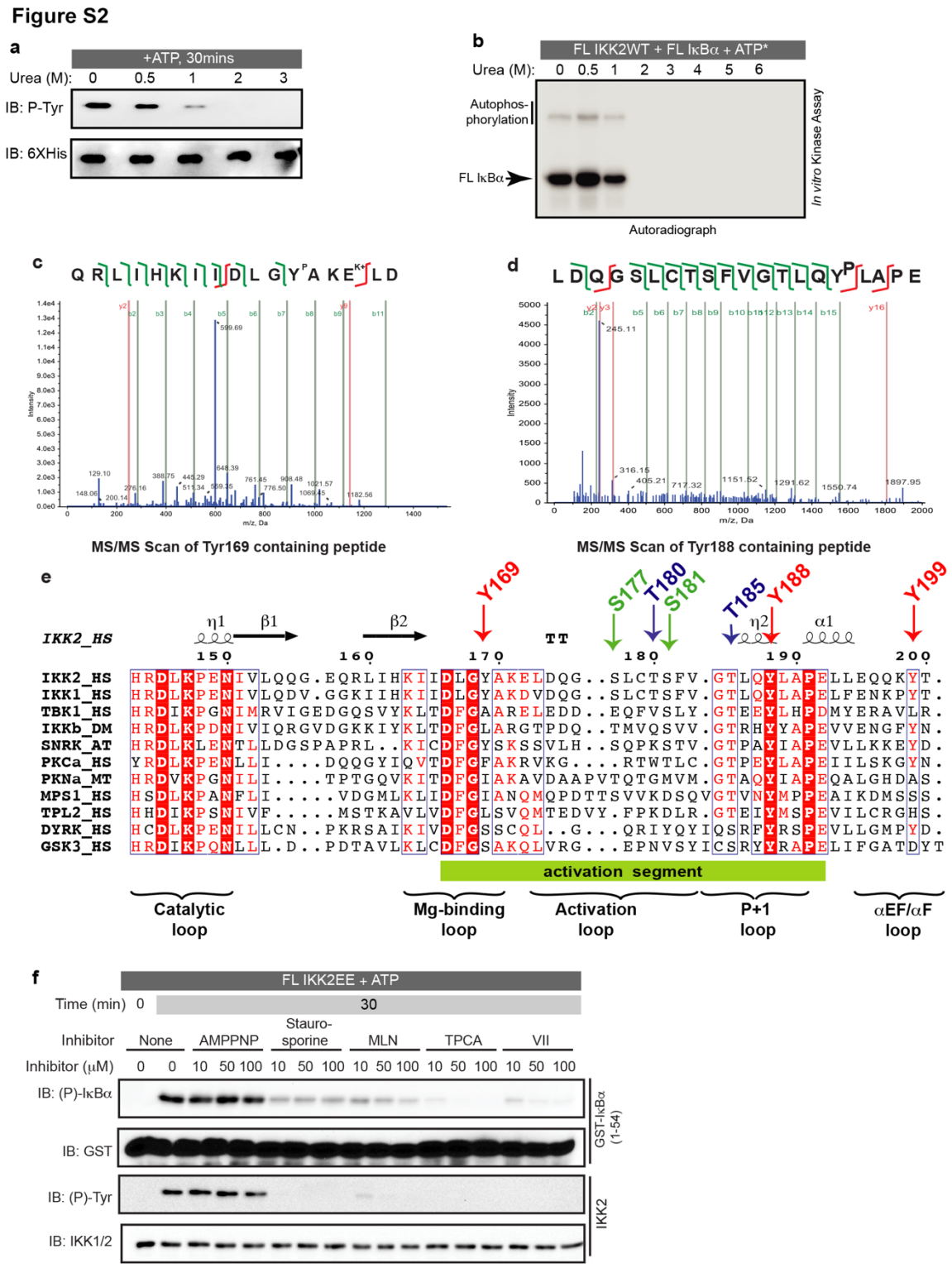

Supplementary Figure 2: a, Effect of increasing concentration of urea on tyrosine autophosphorylation of FL IKK2WT assessed in an *in vitro* kinase assay. **b,** Radioactive *in vitro* kinase assay performed with increasing concentration of urea up to 6M to check auto- and substrate phosphorylation. **c,** Mass spectrometry analysis of ATP-treated IKK2 showing phosphorylation of Tyr169. **d,** Mass spectrometry analysis of ATP-treated IKK2 showing phosphorylation of Tyr188. **e,** Alignment of the activation segment sequences of different IKK family kinases. Conservation of Tyr at the DFG+1 (DLG in case of IKK1 and IKK2) is retained only in a stress response related plant kinase SnRK2, but not in other IKK homologues or any known dual specificity kinases, e.g., DYRK and GSK3β. **f,** Inhibition of both substrate phosphorylation and tyrosine autophosphorylation activities of IKK2 checked in presence of common kinase inhibitors such as AMPPNP and Staurosporine, highly specific IKK2 inhibitors TPCA, Calbiochem Inhibitor VII and MLN120B.

Figure S3

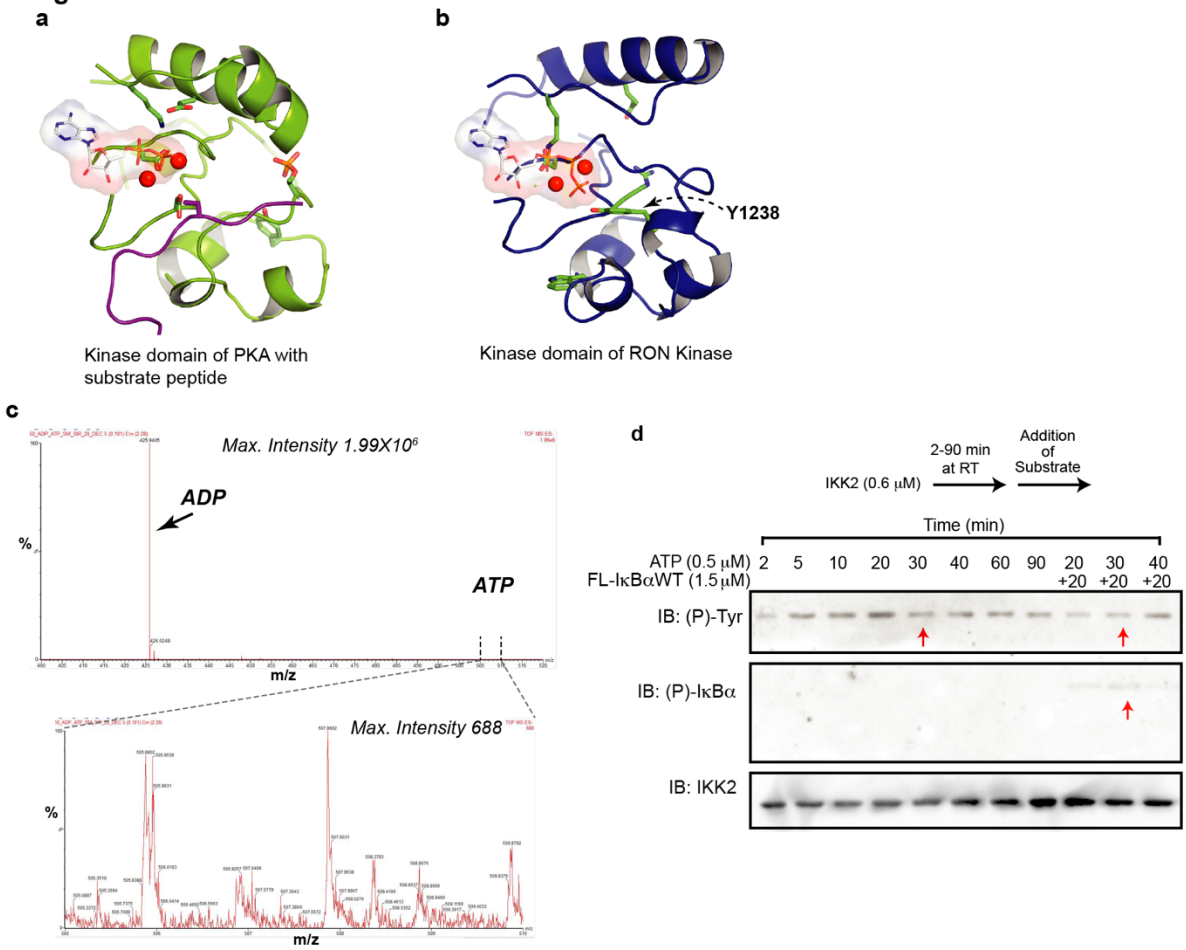

Supplementary Figure 3: a, Substrate bound PKA in its active form; phosphorylatable serine of the substrate peptide (in magenta) is highlighted. **b,** Hydroxyl of Tyr1238 in the activation loop of RON kinase, which is activated through trans auto-phosphorylation, projects towards ATP similarly to that of Tyr169 -OH in IKK2. **c,** ESI-MS scan of the ADP used in this assay system showing negligible trace, if any, of ATP at 50μM ADP concentration. **d,** WB analysis showing auto-phosphorylation of full length IKK2 and phospho-transfer to IκBα.

Supplementary information:

Methods:

Reagents and Cell culture: Monoclonal mouse anti-IκBα (L35A5) (catalogue number: 4814), mouse anti-Phospho-IκBα ($Ser^{32/36}$) (5A5) (catalogue number:9246) and rabbit anti-Phospho-IKKα/β ($Ser^{176/180}$) (16A6) (catalogue number: 2697) were from Cell Signaling Technology (CST). Monoclonal mouse anti-IKKβ (10AG2) (catalogue number: NB100-56509) was from Novus Biologicals. Polyclonal rabbit anti-6XHis (catalogue number: BB-AB0010) was from BioBharti Life Science. Monoclonal mouse anti-Phospho-Tyrosine (catalogue number: 610000) was from BD Biosciences. Polyclonal rabbit anti-GST (catalogue number: 924801), monoclonal mouse anti-HA 11 epitope (catalogue number: 901502) and mouse anti-Tubulinβ3 (catalogue number: 657402) were from BioLegend. Polyclonal rabbit anti-IKKα/β (H-470): sc7607 was from Santa Cruz Biotechnology (has been discontinued) and mouse anti-Phospho-Serine Q5 (catalogue number: 37430) was from Qiagen. Horseradish peroxidase-conjugated secondary antibodies against rabbit (catalogue number: 31460) and mouse IgG (catalogue number: 31430) were Pierce antibodies from Thermo Scientific. Adenosine-5'-Triphosphate (ATP), Disodium trihydrate (catalogue number: A-081-25) was from Gold Biotechnology and Adenosine Diphosphate (ADP) (Reference number: V916A) provided in ADP-Glo™ Kinase assay (catalogue number: V6930) from Promega. Recombinant murine TNF-α used was from Roche.

Sf9 cells used for expressing proteins with baculovirus system was procured from Gibco™ Sf9 cells in Sf-900™ III SFM, Thermo Scientific (catalogue number: 12659017) and maintained in Gibco™Sf-900™ III SFM, Thermo Scientific (catalogue number: 12658019).

Protein expression and purification:

IKK2 (WT and other constructs): Wild-type and mutant IKK2s were purified following a published protocol (Polley et al, 2013). Sf9 cells (Gibco™ Sf9 cells in Sf-900™ III SFM) at a density of 1.5-2 millions/ml were infected with high titre viral stock (generally after P3 stage)

27 at a ratio of 1:100 or 1:50 as optimized for higher expression level as judged by a pilot
28 experiment performed previously, and grown for 48 hours upon infection. Cells were harvested
29 and lysed by sonication in a buffer containing 25 mM Tris-HCl pH 8.0, 200 mM NaCl, 10%
30 Glycerol, 5 mM β-Mercaptoethanol (β-ME), 10 mM Imidazole, 20 mM β-glycerophosphate, 10
31 mM NaF, and 1 mM sodium orthovanadate and 1X Protease Inhibitor Cocktail (PIC, Sigma).
32 The lysate was clarified by centrifugation at 20,000 x g for 45 minutes at 4˚C and incubated
33 with Ni-NTA agarose resin (Qiagen, catalogue number: 30230) pre-equilibrated with lysis
34 buffer for 2 hours at 4˚C. The resin was subsequently washed with lysis buffer containing
35 30mM Imidazole. Protein was eluted with lysis buffer containing 250mM Imidazole. Protein
36 fractions were analysed on SDS-PAGE, pooled together and either flash frozen or subjected
37 to size-exclusion chromatography on Superdex 200 Increase 10/300 GL (GE Healthcare)
38 column equilibrated with 20mM Tris-HCl pH 8.0, 200mM NaCl, 10% Glycerol and 2 mM DTT.
39 To make untagged IKK2, protein fractions eluted from the Ni-NTA resin of desired purity was
40 treated with TEV-protease at a ratio of 50:1 (weight by weight, IKK2: TEV) in the cold room for
41 more than 10 hours after addition of 1 mM of EDTA, the resulting protein mix was then loaded
42 on to the SEC as described above. To prepare autophosphorylated IKK2, the fractions with
43 desired purity level were treated with 0.5-1 mM of ATP,10 mM of $MgCl_2$ and phosphatase
44 inhibitors and the autophosphorylation reaction was carried out at 27˚C for 1 hour. Resulting
45 protein solution was then concentrated in a YM30-concentrator and loaded onto Superdex
46 200 Increase 10/300 GL column. Elution fractions from the size-exclusion step were analysed
47 on SDS-PAGE and peak fractions of desired quality (GE Healthcare) were pooled together
48 and concentrated using a YM30 Centriprep or Centricon devices depending upon the volume
49 of the sample and flash frozen immediately.

50 **IκBα (WT, mutant and other constructs):** His-tagged full length and GST-tagged deletion
51 (1-54) constructs of IκBα (both the wild-type and Ser32Ala, Ser36Ala, Ser32,36Ala single and
52 double-mutant versions) were expressed in *E. coli* Rosetta2 (DE3). The cells were grown
53 overnight at 16˚C after 0.3 mM IPTG induction. The cell pellet was resuspended in 40 ml of

54 Lysis Buffer (25 mM Tris pH 7.5, 200 mM NaCl, 10 mM imidazole, 10% Glycerol, 5 mM β-
55 mercaptoethanol, and 1 mM PMSF). The cells were lysed by using sonicator keeping the cell
56 suspension chilled on ice. The lysate was clarified by centrifugation at 15,000 x g for one hour
57 at 4°C. About 3 ml of Ni-NTA Agarose resin was equilibrated with lysis buffer, and the clarified
58 lysate (supernatant) was mixed with it later. The protein was allowed to bind the resin by
59 incubating for 2 hours on a rotary mixer in a 4°C room. The resin was washed with the lysis
60 buffer containing 500 mM NaCl (high salt wash) for about 10 CV to clear out non-specific
61 proteins from binding. Then the resin was thoroughly washed with the lysis buffer containing
62 20 mM imidazole. His-tagged IκBα protein was eluted under gravity flow, using elution buffer
63 (the lysis buffer containing 250 mM imidazole). ~1 ml volume of each fraction was collected.
64 (For GST tagged proteins, Glutathione Sepharose resin (GE Healthcare, catalogue number:
65 17-5279-01) was used and elution was performed with the help of reduced glutathione). The
66 main elution fractions were subjected to size-exclusion chromatography (SEC) on a HiLoad
67 16/600 pg Superdex 200 column (GE Healthcare) and the gel run revealed cleaner protein
68 fractions. The peak fractions were saved and stored at -80˚C.
69 **NEMO (WT, mutant and other constructs):** NEMO FL, NEMO double mutant C76A C95S
70 (site directed mutagenesis done in pET24d vector) and NEMO (44-196) (truncates in pET24d)
71 were expressed in *E. coli* Rosetta2 DE3 cells. The cells were grown overnight at ~21˚C after
72 0.25 mM IPTG induction (at 0.3-0.4 O.D.) and 50-100 μM Zn^{2+}. [OR The cells were grown
73 overnight (~17 hours) at 16˚C after 0.1 mM IPTG induction (at 0.2-0.3 O.D.) and 50-100 μM
74 Zn^{2+}]. The cell pellet was resuspended in 40 ml of Lysis Buffer (25 mM Tris pH 7.5, 200 mM
75 NaCl, 10 mM imidazole, 10% Glycerol, 5 mM β-mercaptoethanol, 20μM $ZnCl_2$, 0.5 M urea
76 (acting like an osmolyte). Rest of the steps performed were typical to a Ni-NTA purification as
77 described above. The main elution fractions were subjected to size-exclusion chromatography
78 on a HiLoad 16/600 pg Superdex 200 column (GE Healthcare) and the cleaner peak fractions
79 were stored at -80˚C.

80 **Kinase Assay with purified proteins:** Typically, 100-200 ng (unless mentioned otherwise)
81 of purified kinase was used in each *in vitro* kinase reaction. 0.5-1μg of IκBα substrate (full-
82 length or GST-tagged 1-54) was incubated with kinase for 30 mins or indicated time periods
83 at 27˚C in presence of 20μM ATP with 0.1μCi of γ-P32-ATP in case of radioactive assay or
84 50-100 μM ATP in case of Western blot assay in a reaction buffer containing 20mM HEPES
85 pH 7.5, 100mM NaCl, 15mM $MgCl_2$, 2mM DTT, 0.2mM Na_3VO_4, 10mM NaF, 20mM β-
86 Glycerophosphate. Reaction was stopped by heating the samples at 95˚C for 5 mins after the
87 addition of 1X-Laemmli buffer. Samples were run on 8 or 10% SDS-PAGE. For radioactive
88 assays, the gel was then dried and analysed either by film or phosphor-imaging. For Western
89 blot assays, proteins from gel were electro-transferred onto nitrocellulose/PVDF membrane
90 and probed with desired antibodies. Phosphorylated tyrosine and serine residues were
91 detected using monoclonal antibodies against phospho-tyrosine and phospho-serine.

92 **IP-Kinase assay:** Immortalized *ikk2*$^{-/-}$ mouse embryonic fibroblast 3T3 cells were
93 reconstituted by retroviral transduction with HA-tagged WT or mutant pBABE-IKK2 constructs.
94 Stable expression of IKK2 was first confirmed by immunoblotting. Cells were then stimulated
95 with recombinant murine TNF-α (Roche) at 70-80% cell confluency. IKK complex was
96 immunoprecipitated from whole cell extracts using a NEMO-specific antibody (BD) and Protein
97 A agarose (Upstate) for 2 hrs in the cold room. Whole cell extract used was pre-cleared by
98 incubation with Protein A agarose bead for an hour. Immunoprecipitated complex was washed
99 extensively, including a final washing step with the kinase assay buffer devoid of ATP and
100 incubated with GST-IκBα (1-54) and 20 μM ATP and 5 μCi of γ32P-ATP for 30 mins at 30˚C
101 in kinase assays. Reactions were stopped by addition of 2X-Laemmli SDS buffer to samples
102 and heating at 95˚C for 5 mins. Reaction products were resolved on a 12% SDS PAGE. Extent
103 of substrate phosphorylation was measured by cutting out the appropriate area of the gel
104 containing the substrate and subjecting it to phosphor-imaging (Typhoon, GE Life Sciences)
105 after drying. As a control, amount of IKK2 in each reaction was estimated by transferring IKK2
106 containing gel area onto nitrocellulose membrane and probing it with anti-IKK1/2 antibody.

107 **Sample preparation for LC-MS/MS analyses for Tyrosine phosphorylation detection:**
108 Protein samples were diluted in TNE (50mM Tris pH 8.0, 100mM NaCl, 1mM EDTA) buffer.
109 RapiGest SF reagent (Waters Corp.) was added to the mix to a final concentration of 0.1%
110 and samples were boiled for 5 min. Tris (2-carboxyethyl) phosphine (TCEP) was added to a
111 final concentration of 1mM and the samples were incubated at 37˚C for 30 min. Subsequently,
112 the samples were carboxymethylated with 0.5 mg/ml of iodoacetamide for 30 min at 37˚C
113 followed by neutralization with 2mM final concentration of TCEP. Proteins samples prepared
114 as above were digested with trypsin (trypsin: protein ratio - 1:50) overnight at 37˚C. RapiGest
115 was degraded and removed by treating the samples with 250 mM HCl at 37˚C for 1 h followed
116 by centrifugation at 14000 rpm for 30 min at 4˚C. The soluble fraction was then added to a
117 new tube and the peptides were extracted and desalted using C18 desalting columns (Thermo
118 Scientific).

119 **LC-MS/MS analysis:** Trypsin-digested peptides were analysed by ultra-high-pressure liquid
120 chromatography (UPLC) coupled with tandem mass spectroscopy (LC-MS/MS) using nano-
121 spray ionization. The nano-spray ionization experiments were performed using a TripleTOF
122 5600 hybrid mass spectrometer (ABSCIEX) interfaced with nano-scale reversed-phase UPLC
123 (Waters corporation nano ACQUITY) using a 20 cm-75-micron ID glass capillary packed with
124 2.5 µm C18 (130) CSHTM beads (Waters corporation). Peptides were eluted from the C18
125 column into the mass spectrometer using a linear gradient (5–80%) of Acetonitrile (ACN) at a
126 flow rate of 250 µl/min for 1h. The buffers used to create the ACN gradient were: Buffer A (98%
127 H2O, 2% ACN, 0.1% formic acid, and 0.005% TFA) and Buffer B (100% ACN, 0.1% formic
128 acid, and 0.005% TFA). MS/MS data were acquired in a data-dependent manner in which the
129 MS1 data was acquired for 250ms at m/z of 400 to 1250 Da and the MS/MS data was acquired
130 from m/z of 50 to 2,000Da. The Independent data acquisition (IDA) parameters were as
131 follows; MS1-TOF acquisition time of 250 milliseconds, followed by 50 MS2 events of 48
132 milliseconds acquisition time for each event. The threshold to trigger MS2 event was set to
133 150 counts when the ion had the charge state +2, +3 and +4. The ion exclusion time was set

134 to 4 seconds. Finally, the collected data were analysed using Protein Pilot 4.5 (ABSCIEX) for
135 peptide identifications.

136 **ESI-MS analyses of ADP:** 50 μM of ADP solution was prepared to be analysed by
137 Electrospray Ionisation Mass Spectrometry (ESI-MS). It was performed in a Xevo G2-XS QToF
138 mass spectrometer (Waters Corporation) using capillary at 3kV, with voltage parameters of
139 sampling cone at 40V and source offset at 80V. The source temperature was set at 100˚C and
140 desolvation temperature at 40˚C. The gas flow rates were as follows: Cone gas flow rate at 50
141 litre/hr and desolvation gas flow rate at 400 litre/hr. The sample was passed at 5 μl/min flow
142 rate. The MS data was acquired for a mass range of 50-2000 m/z and the acquisition time was
143 1 minute.

144 **Radioactive Phosphotransfer assay:** Phosphotransfer assays were performed in a wide
145 range of concentration of IKK2, IκBα and ATP. Typically, 10 μM purified IKK2 protein was first
146 autophosphorylated in presence of 100-200 nM of γ32P-ATP (PerkinElmer) in kinase assay
147 buffer for 1 hour at 30˚C. 70 μl of the resulting reaction mixture was first passed through a
148 Micro Bio-Spin Bio-Gel P-30 spin column (Bio-Rad; 40 kDa MWCO) equilibrated with 20 mM
149 HEPES pH 7.9, 100 mM NaCl, 0.2 mM Na_3VO_4, 10 mM NaF, 20 mM β-Glycerophosphate, 2
150 mM DTT, 2 mM EDTA and 1X protease inhibitor cocktail. Eluted protein was subjected to
151 another round of buffer exchange on a Bio-Gel P-30 column equilibrated with the same buffer
152 mentioned above devoid of EDTA and containing 15 mM $MgCl_2$. Phosphorylated IKK2 thus
153 obtained was used in phosphotransfer reaction. 2-3 μM of Phosphorylated IKK2 was
154 incubated with 10-20 μM of WT or mutant IκBα protein at 30˚C in kinase assay buffer in a total
155 volume of 20 μl for different time periods as indicated in Figure 3b and 4a. The reactions were
156 stopped by addition of 10 μl of 4X Laemmli SDS-buffer containing 100 mM EDTA to samples
157 and heating at 95˚C for 5 mins. Different concentration of ADP or ATP was added to the assay
158 to assess the role of these nucleotides in phosphotransfer efficiency. Routinely, 10-15μl of
159 reaction products were resolved on 10% SDS PAGE and radiolabelled samples were
160 monitored by phosphor imaging of the dried gel on a Typhoon scanner. For the

161 phosphotransfer reaction described in Figure 4a, 10 μM purified IKK2 was autophosphorylated
162 with of 100 nM of γ^{32}P-ATP in presence of 40 μM of cold ATP.

163 **Phospho-transfer assay with cold ATP:** About 10 μM of purified FL IKK2WT was treated
164 with 100 μM of cold ATP in kinase assay buffer (containing 1X protease inhibitor cocktail) for
165 one hour at 30˚C. The resulting reaction mixture was then loaded onto a Superdex 200
166 increase 10/300 GL (24ml bed volume, Cytiva) SEC column to purify autophosphorylated FL
167 IKK2WT separated from excess ATP. SEC was performed in buffer containing 20 mM HEPES,
168 100 mM NaCl, 20 mM β-glycerophosphate, 10 mM NaF, 0.2 mM Na3VO4 and 2 mM DTT.
169 The elution fractions containing phosphorylated IKK2 were incubated with FL IκBαWT in
170 presence of different concentrations of ATP or ADP at different time points (as mentioned in
171 Figure 3f) at 30˚C. The reactions were stopped by adding 4X Laemmli SDS dye, heated at
172 95˚C for 5 minutes and were run on a 10% SDS-PAGE. This was followed by immunoblotting
173 and detection was done using monoclonal antibodies against phospho-tyrosine and phospho
174 $Ser^{32/36}$ IκBα.

175

176

177

178

179

180

181

182

183

184